Comparison of laser ablation, electrothermal vaporization and solution nebulization for the determination of radionuclides in liquid samples by inductively coupled plasma mass spectrometry

Grinberg, P.; Yang, L.; Mester, Z.; Willie, S. N.; Sturgeon, R.

Publisher's version / Version de l'éditeur:
https://doi.org/10.1039/b607911c
Journal of Analytical Atomic Spectrometry, 21, 11, pp. 1202-1208, 2006

Comparison of laser ablation, electrothermal vaporization and solution nebulization for the determination of radionuclides in liquid samples by inductively coupled plasma mass spectrometry

Patricia Grinberg,* Lu Yang, Zoltan Mester, Scott Willie and Ralph E. Sturgeon

Received 5th June 2006, Accepted 16th August 2006
First published as an Advance Article on the web 4th September 2006
DOI: 10.1039/b607911c

The performance of solution nebulization (SN), electrothermal vaporization (ETV) and laser ablation (LA) of dried micro-droplets as sample introduction systems for ICP-MS are compared for the determination of several radionuclides in digested biological tissue, nearshore sea-water and river water. Samples were subjected to a $Ca_3(PO_4)_2$ co-precipitation preconcentration prior to analysis. Each introduction system possesses unique advantages and disadvantages. ETV accommodates samples having higher dissolved solids content; consequently, for SN and LA, sample concentrates require additional dilution by 50- and 10-fold, respectively. ETV and LA achieved similar sensitivities and limits of detection, the latter ranging from 0.017 to 0.029 pg ml^{-1}. Although SN provides the best precision (2% RSD *versus* 7 and 8% for ETV and LA, respectively), formation of uranium hydride can be reduced at least 100-fold using LA of dried micro-droplets of samples. The accuracy of the method was validated by determination of U and Th in NIST SRM 1566b Oyster Tissue, NRC CRM CASS-4 Nearshore Seawater and SLRS-4 Riverine Water and *via* spike recoveries for Pu.

Introduction

Radiochemical methods[1–4] requiring careful and time consuming separation and enrichment processes with intensity measurements of characteristic α- β- or γ-emitting species constitute the traditional techniques for quantitation of radionuclides in the nuclear sciences. However, routine use of mass spectrometry has been increasing over the past 15 years. Amongst these mass spectrometric approaches, accelerator mass spectrometry (AMS), thermal ionization mass spectrometry (TIMS) and inductively coupled plasma mass spectrometry (ICP-MS) are the most popular,[5–8] with ICP-MS becoming more frequently used.

By far the most common radioisotopes measured by ICP-MS are the long-lived actinides, principally ^{238}U and ^{232}Th, although Pu isotopes, ^{237}Np and ^{99}Tc are also now more frequently addressed in environmental and nuclear applications due to the improvements in analytical performance of the newer generation of ICP-MS instrumentation. Since actinide concentrations are typically very low in most environmental applications [often in the sub-pg to pg (kg or L)$^{-1}$ range], their detection presents a significant challenge for ICP-MS, prompting the development of new and innovative approaches to sample preparation and introduction. A variety of solution nebulization (SN) systems,[9–12] as well as electrothermal vaporization (ETV)[13–17] and laser ablation (LA)[18] techniques have thus been examined, the latter two holding promise of increased detection power because of enhanced sample introduction efficiency and, frequently, lower background arising from molecular ions. In addition, ETV has the ability to use thermal programming, allowing selective removal of sample matrix constituents, thereby eliminating or reducing spectroscopic interferences that would otherwise arise from the matrix. Isobaric interferences can also be reduced/eliminated or compensated for with the use of high-resolution spectrometers, mathematical corrections, chemical separation and by taking advantage of selective ion–molecule reactions using a reaction or collision cell.

We have earlier evaluated[17] the use of ETV sample introduction for the determination of U, Th and Pu in natural water, biological materials and urine. These elements suffer strong interaction with the graphite substrate at high temperatures, leading to carbide formation, severe memory effects and poor sensitivity. This problem can be circumvented with the use of sample vaporization from a tantalum surface and addition of a gaseous (Freon) modifier. The resultant dry plasma reduces signal intensities for all H-, O- and OH- based molecular ions, decreasing analyte hydride formation and molecular/polyatomic interferences.

LA-ICP-MS has been widely used for micro-sampling of solids for geological,[18,19] biological,[20,21] environmental,[22,23] nuclear[24] and metallurgical[25,26] applications. Despite several advantages, including μg g^{-1} detection limits and direct access to analytes in solid matrices, quantitative analysis remains problematic due to the lack of matrix-matched solid standards for calibration. Alternative calibration strategies have thus been developed, such as co-nebulization of standard solutions,[25,27–29] but the different ablation characteristics of solid samples frequently leads to matrix effects[30] and elemental fractionation.[31,32] Unfortunately, under such circumstances,

Institute for National Measurements Standards, National Research Council Canada, Ottawa, Ontario, Canada K1A 0R6. E-mail: patricia.grinberg@nrc.ca; Fax: +1-613-993-2451

solution calibration cannot be used. Recently,[33] LA for the quantitative analysis of dried micro-droplets with detection limits in the low-ppb range was reported for Ni, Cd and Pb. Analyte quantitation by complete ablation of micro-droplets appears to avoid many of the pitfalls of conventional micro-sampling by LA, including the need for matrix matched certified reference materials and concerns over elemental fractionation, while retaining the benefits of SN—namely the ability to easily undertake isotope dilution calibration or improve precision by addition of other internal standards.

The aim of this study was to compare the performance of SN, ETV and LA of dried micro-droplets as complimentary analyte introduction techniques for analysis of actinides in environmental samples. The advantages and disadvantages of these three approaches are highlighted by the determination of Th, U and Pu in water, digested biological materials and spiked matrices (for Pu).

Experimental section

Instrumentation

A quadrupole ICP-MS (ELAN DRC II ICP-MS, PerkinElmer SCIEX, Shelton, CT) was operated in standard mode, in that no alternative gas was added to the reaction cell. For SN, a cyclonic glass spray chamber and a Meinhard nebulizer were used.

For ablation of dried microdroplets of samples, a frequency quadrupled Nd-YAG laser system operating at 266 nm [UP266MACRO (New Wave Research, California, USA)] and 3.4 mJ (100% energy) was used. A laser spot size of 900 μm was used with a scanning speed of 900 μm s^{-1} (when raster scanning was studied). Data acquisition on the ELAN DRC II was manually triggered prior to ablation of the samples. The intensities of the analytes were simultaneously monitored and the acquired data were processed using in-house software.

For ETV sample introduction, a PerkinElmer HGA-600MS electrothermal vaporizer fitted with a Model AS-60 auto-sampler housed in a HEPA filtered cabinet to minimize contamination from the laboratory atmosphere was used. Pyrolytic graphite-coated tubes fitted with a tantalum insert,[17] along with trifluoromethane (1.4% Freon-23 in Ar) (Air Liquide Canada Inc.) as a gaseous modifier, were used. The ETV was operated under software control from the host ELAN computer.

The transfer line between the LA cell/ETV and the base of the ICP torch was an 80 cm long, 6 mm id Teflon lined Tygon tube (Cole-Parmer Instrument Co., IL) flushed by the ICP-MS carrier gas flow. Peak areas were used for the final quantitation of analyte concentrations by LA and ETV sample introduction.

Sample aliquots were deposited and dried on polystyrene weighing boats (VWR International, Mississauga, Ontario, Canada), which were used as substrates for the LA studies.

All plastic and glassware were cleaned by immersion in 50% (v/v) HNO_3 for at least 24 h and thoroughly rinsed with Milli-Q water before use. A microwave digestion system (CEM Model MDS 2100, Mattiews, NC, USA) was used for digestion of oyster tissue samples.

Reagents and solutions

High purity deionized water (DIW) was produced by reverse osmosis of tap water followed by deionization (Barnstead/Thermolyne, Dubuque, IA, USA) to yield 18 MΩ cm resistivity reagent.

Stock solutions (1000 mg l^{-1}) of Th and U were prepared by dissolution of appropriate masses of the respective nitrate salts. A 1.25 μg L^{-1} stock solution of ^{242}Pu was prepared from NIST SRM 4334G (Gaithersburg, MD, USA). Working standards were prepared just before use by serial dilutions of the stock solution using DIW. Lutetium was used as an internal standard for LA.

Nitric acid was purified in-house prior to use by sub-boiling distillation of reagent grade feedstock in a quartz still. All other chemicals were of analytical reagent grade. Industrial grade He and Ar (Praxair Products Inc., Mississauga, ON) were used throughout.

Certified Reference Materials NIST SRM 1566b Oyster Tissue (Gaithersburg, USA), NRCC (National Research Council Canada) CASS-4 Nearshore Seawater and SLRS-4 Riverine Water reference materials for trace metals were used for validating the accuracy of the proposed methods.

Sample treatment

Digestion of oyster tissue. A nominal 0.25 g sample was accurately weighed into a CEM Teflon digestion vessel and 7 ml of HNO_3 were added. The vessel was capped and the sample digested using microwave heating at a pressure of 120 psi for 30 min. After cooling, 200 μl of H_2O_2 (30%) was added, the vessels were recapped and heated again using the same microwave program. The digestate was then cooled and diluted to 50 ml with DIW.

Co-precipitation procedure. Calcium phosphate co-precipitation was used to achieve matrix separation and analyte preconcentration[17] for all samples and standards, unless stated otherwise. A 50 ml aliquot of sample was pipetted into a polypropylene centrifuge tube followed by addition of appropriate standards. A 50 μl volume of 0.125 M $Ca(NO_3)_2$, 2 drops of phenolphthalein indicator and 200 μl of 0.32 M $(NH_4)_2HPO_4$ were then added. Concentrated NH_4OH was slowly added until the phenolphthalein end point was reached and precipitation of $Ca_3(PO_4)_2$ occurred. The solution was shaken for 2 min and then centrifuged for 10 min at 3000 rpm. The supernatant fluid was decanted and the precipitate dissolved in 1 ml of 5% HNO_3. This concentrate is compatible with direct analyses by ETV whereas 50- and 10-fold dilutions were required for SN and LA, respectively.

Sample introduction by LA. For sample introduction by LA, dried micro-droplets of the sample were examined. Multiple 20 μl volumes of sample were deposited onto a polystyrene weighing boat, which was then placed in a class-10 fume hood on a hot plate under an IR lamp. When the droplets were dry, the bottom of the weighing boat was then excised and inserted into the LA sampling chamber for ICP-MS analysis.

The addition of Lu as an internal standard (IS) to solutions subjected to LA served to enhance the resulting precision. Although not used as a conventional IS in that no effort was made to match the ionization potential or atomic weight of IS to those of the analytes, the precision of replicate measurements was enhanced about 3-fold. The presence of Lu served to account, to some degree, for variation in the LA yield.

Sample introduction by ETV. During the sample drying and pyrolysis steps, opposing 300 ml min^{-1} flows of argon originating from both ends of the graphite tube remove water and other vapors through the dosing hole. During the high temperature vaporization step, the dosing hole is sealed (2 s prior to this step) by a pneumatically activated graphite probe. Once sealed, a valve located at one end of the HGA workhead directs the carrier argon gas flow originating from the opposite end of the graphite tube directly to the ICP. Total carrier gas flow rate was maintained at 1000 ml min^{-1}, irrespective of contributions from internal purge gas flows. A 20 µl volume of the calibration solution or sample was automatically delivered to the tube for all measurements. The furnace was maintained at room temperature during the injection of samples.

Sample introduction by SN. For sample introduction by SN, a cyclonic glass spray chamber and a Meinhard nebulizer were used. Compared with both ETV and LA sample introduction systems, steady-state signals permitted longer dwell times (50 ms) to be used for SN, increasing the integrated ion count to yield improved precision and detection limits.[34]

Results and discussion

ICP-MS operating conditions and sample introduction parameters are summarized in Table 1. As the concentration of the actinides in the samples can reach extremely low concentrations (*i.e.*, low pg g^{-1} levels), preconcentration was essential for detection. This was achieved by undertaking a co-precipitation of U, Th and Pu with calcium phosphate.[17]

Optimization of response

Initial optimization of the plasma and mass spectrometer was achieved using solution nebulization but all operating parameters (rf power, nebulizer Ar flow rate, lens voltage) were optimized for all three sample introduction systems in order to obtain maximum sensitivity for the analytes and minimum signal for doubly charged ions, oxides and background. Similar conditions arose for all sampling systems.

Samples were analyzed following co-precipitation. As a high dissolved solids content arises from use of this procedure, no preconcentration could be used for SN studies.

With ETV, samples were vaporized from the surface of a 10 mm long Ta insert placed in the graphite tube. This process was aided by use of a tetrafluoromethane (Freon-23) gaseous modifier to minimize carbide formation.[17] A lifetime of about 160 firings could be achieved for each Ta insert. Memory effects were observed when analyzing samples having concentrations of U higher than 5 ng g^{-1}. In such case, a blank was run after each sample to ensure no carryover.

Previous work[33] revealed that ablation of dried microdroplets of samples can be used for the quantitative determination of Ni, Cd and Pb in water samples. The drying procedure determines the size and shape[35] of the residue, ideally a spot having a diameter smaller than the focused laser beam diameter. Dried residues derived from calibration solutions ranged in size from 100–400 µm, permitting the entire deposit to be ablated using a single shot. Unfortunately, with real samples, dried residue diameters were as large as 1.3 mm and required multiple laser shots to achieve complete ablation. Samples dried using an infrared lamp provided a homogeneous appearance. Residues derived from digested oyster tissue (without $Ca_3(PO_4)_2$ precipitation) exhibited an irregular shape with maximum dimensions of about 1.6 mm.

The distribution of the analytes and the internal standard within the dried residue was investigated by dividing the spot into approximately 150 sub-regions and examining the material using a laser spot size of 5 µm (energy of 3.4 mJ, the UP266 MACRO has an internal aperture wheel to control the beam size while maintaining constant energy density). Fig. 1 shows a typical contour map illustrating the distribution of U and Lu (internal standard) in a dried droplet of sea-water following co-precipitation with $Ca_3(PO_4)_2$. Each line traces an isoconcentration (% relative) and the relative density of lines reflects relative changes in concentration. As is evident from the circular distribution, the highest analyte concentration (for both U and Lu) can be found along the rim of the dried sample with the lowest in the middle. During drying, salt precipitates prior to complete evaporation of the droplet, forming the circular pattern. The partitioning of the analyte into different regions of the spot can result in variation in the sampling of all components. The same characteristics were observed for the digested oyster tissue sample. It is evident that, unless

Table 1 Operating conditions

ICP-MS system	
Rf power	1100 W
Auxiliary Ar flow rate	1.2 l min^{-1}
Nebulizer Ar flow rate	1.05 l min^{-1} (1.0 l min^{-1} for ETV)
Plasma Ar flow rate	15 l min^{-1}
Peak scan parameters	
m/z per reading cycle	(^{238}U, ^{232}Th, ^{242}Pu)
Dwell time	30 ms (LA and ETV), 50 ms (SN)
Sweeps per reading	1 (LA and ETV), 20 (SN)
Readings per replicate	300 (LA and ETV), 1 (SN)
No. of replicates	1 (LA and ETV), 10 (SN)
Measurement mode	Peak hopping
SN unit	
Spray chamber	Cyclone, glass
Nebulizer	Meinhard
Sample flow rate	1 ml min^{-1}
LA unit	
Repetition rate	20 Hz
Energy per pulse	3.4 mJ
Scanning speed/µm s^{-1}	900
Spot size/µm	900
Signal measurement	Peak area
ETV unit	
Drying temperature/°C	120, ramp 10 s, hold 20 s
Pyrolysis temperature/°C	1200, ramp 10 s, hold 20 s
Vaporization temperature/°C	2300, 10 s
Cleaning temperature/°C	2650, ramp 1 s, hold 5 s
Sample volume/µl	20
Modifier	Tantalum insert and 1.4% Freon-23 in Ar
Signal measurement	Peak area

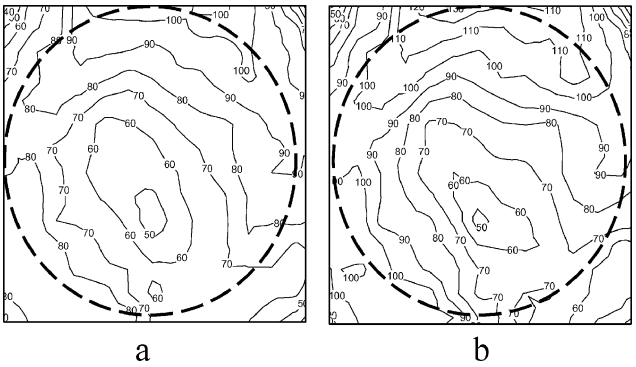

Fig. 1 Concentration contours for (a) U and (b) Lu (internal standard) showing the relative distribution of each element (normalized to its maximum) over a dried droplet of sea-water subjected to $Ca_3(PO_4)_2$ co-precipitation. The broken line indicates the initial location of the liquid spot.

complete ablation is achieved, the advantages of use of the internal standard are obviated.

As the diameters of sample deposits exceeded the laser spot size available and because of the inhomogeneous analyte distribution across the dried sample, an area encompassing the entire spot was raster ablated at 900 μm s^{-1} and integrated intensities calculated.

Despite reports to the contrary,[36,37] the influence of an added flow of He (constituting up to 70% of the nebulizer gas flow) to the laser ablation cell produced no improvement in sensitivity or precision. Pure argon was thus used as a carrier at 1.05 L min^{-1}.

Fig. 2 illustrates typical signals obtained with ETV and LA introduction systems for a sea-water sample (CASS-4) subjected to the calcium phosphate co-precipitation procedure. LA profiles resemble those arising with ETV sample introduction. Typical half-widths are about 3 and 1 s for LA and ETV, respectively. The main process dictating the duration of the signal profile for LA is not the ablation process, but the subsequent transport of aerosol from the LA cell to the plasma, similar to the situation with ETV.[38] The relative appearance times for the signals in Fig. 2 are not relevant because of inconsistencies in the start of data acquisition. Note, however, the enhanced tailing in the ETV signal because of extended interaction of the U with the hot graphite.

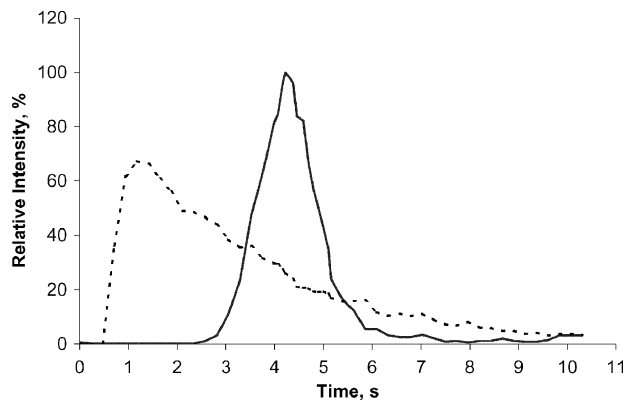

Fig. 2 Temporal signal profile for U obtained for a sea-water sample (CASS-4) subjected to co-precipitation procedure using (—) ETV and (···) LA introduction systems.

Figures of merit

Analytical figures of merit obtained using SN, LA and ETV sample introduction are summarized in Table 2 and pertain to samples, which were subjected to the calcium phosphate co-precipitation procedure.

Different peak scan parameters were used for SN, ETV and LA. ETV and LA measurements produce transient signals lasting 4 and 8 s, respectively. As quadrupole mass spectrometers sequentially acquire m/z data, different peak scanning parameters are required for transient signals in order to collect sufficient counts to optimize S/N ratios. Dwell times are influenced by several parameters, including the number of isotopes monitored and the signal peak width. In this study, scan parameters for both LA and ETV were chosen in order to ensure that the signal transients were characterized by at least 10 sampling intervals over their duration.[39]

When using ETV, a 10- and 50-fold higher enrichment factor could be achieved compared with LA and SN, respectively, because ETV can accommodate the resultant higher dissolved solids content. Preconcentration could not be used with SN in order to avoid injector salting problems. Attempts to utilize concentrated samples with LA (using the same LA settings shown in Table 1) resulted in incomplete ablation with a significant fraction of the sample being removed from the surface and deposited on its surroundings.

Detection limits are based on a 3 s criterion, where s is the estimated standard deviation of at least 7 repetitive measurements of a procedural blank. Blanks were prepared by subjecting 50 ml DIW (0.5% HNO_3) to the co-precipitation procedure.

LA provided detection limits 2-fold worse than ETV, likely due to incomplete ablation. If a chromogenic matrix [5 μl volume of 500 ppb of *trans*-2-(3-(4-*tert*-butylphenyl)-2-methyl-2-propenylidene) malonitrile)] was added to the sample, LODs were similar to those for ETV and about 5-fold better than achieved with SN. Such matrices may serve to enhance the UV absorption efficiency of the laser beam (as used in MALDI applications), thereby increasing the ablation efficiency, but

Table 2 Figures of merit

	SN	LA	ETV
LOD/pg ml^{-1}[a]			
U	0.12	0.072	0.029
Th	0.13	0.051	0.013
Pu[b]	0.12	0.033	0.017
Sensitivity/counts[c]			
U	35 600 ± 400	103 000 ± 4000	128 000 ± 6000
Th	36 700 ± 600	92 000 ± 3000	153 000 ± 9000
Pu	39 600 ± 400	96 000 ± 3000	120 000 ± 5000
EF[d]	0	5	50
Precision (% RSD)[e]	2	8	7

[a] Data corrected for preconcentration factors (n = 7). [b] Based on ^{242}Pu spike measurements. [c] For 20 pg analyte (n = 3). [d] EF = enrichment factor. [e] n = 10.

may equally well influence response by altering the transport characteristics of the aerosol.

Absolute sensitivities (response for 20 pg) for U, Th and Pu are presented in Table 2. For SN the signal was integrated for a specific time at a known introduction rate (1 ml min^{-1}) to provide an estimate of the absolute mass of analyte "injected" (not accounting for introduction efficiency). Sensitivities are enhanced 1.3- and 3.5-fold using ETV compared with LA and SN, respectively, whereas LA provides a 2.5-fold enhancement over SN. Higher SN sensitivities could possibly be achieved using more efficient devices, such as microconcentric and ultrasonic nebulizers.[12]

Precision, expressed as a relative standard deviation for 10 consecutive replicates at analyte concentrations approximately 100-fold higher than the procedural LOD, was evaluated for each introduction system. Precision was poorer for LA and ETV than for SN and can be attributed to variability in the vaporization/ablation processes for replicate analyses. No significant difference was evident between ETV and LA (7 and 8%, respectively). No significant background (less than 100 cps) was detected for the target analytes during ablation of an unloaded polystyrene substrate.

For LA, as expected, use of smaller laser spot sizes (simulating different LA systems) deteriorated precision. With a 400 μm laser beam diameter (3.4 mJ energy), precision deteriorated from 8 to 12%, mainly due to the need for additional shots to ensure complete sample ablation and consequently a longer integration time.

Sample throughput is superior with SN. One sample/standard pair can be processed in about 3 min (considering 3 replicates) using co-precipitated calibration standards for quantitation. Although ETV can be readily programmed to permit selective removal of sample matrix constituents and eliminate or reduce spectroscopic interferences that would otherwise arise from the matrix, the analysis time is lengthy. Similar to SN, co-precipitated calibration standards were used for quantitation and the analysis time for a single sample/standard is about 9 min (considering 3 replicates). Throughput could likely be significantly enhanced using a multiplexing approach recently described by Venable *et al.*[40]

Table 3 Hydride formation using different sample introduction systems. (n = 3)

Sample introduction system	UH^+/U^+	Ref.
Laser ablation	1.8×10^{-8}	This work
ETV	2.5×10^{-6}	17
SN (Meinhard)	1.3×10^{-5}	42
SN (Meinhard) using D_2O	2.6×10^{-7}	42
SN with desolvation (CETAC Aridus)	1.0×10^{-5}	9

The method of standard additions was used for quantitation by LA, providing a sample throughput of about 15 min per sample/standard (considering 3 replicates and 3 calibration points). External calibration with matrix matching could not be used with LA as samples contained varying amounts of calcium, which influenced response. The time required for drying droplets is not considered in this estimate of throughput. Preparation of the samples by drying under an IR lamp takes about one hour, but this could easily be multiplexed, which would then not present a limiting factor for throughput. Moreover, enhanced throughput could be achieved using automated spotting/drying techniques common to MALDI.[41] The use of a smaller volume ablation cavity, as currently used in MALDI instruments, would also be attractive for optimum transient generation.

One of the most significant problems relating to the determination of Pu (more specifically ^{239}Pu) is interference due to the formation of UH when high concentrations of U are present. Several approaches, including use of different nebulizers,[9,42,43] analyte separation[44] and substitution of D_2O for H_2O as solvent[9,42] have been used in efforts to reduce hydride formation. Table 3 summarizes the relative UH^+/U^+ ratios obtained with the different sample introduction approaches. When using LA or ETV, the dry plasma considerably reduces the signal intensities of all H-, O- and OH-based molecular ions compared with those obtained with a wet plasma. Hydride formation is reduced at least 2 orders of magnitude with LA compared with the other sample introduction systems, which should significantly improve the reliability of determination of ^{239}Pu.

Table 4 Analysis of samples. (n = 3)

	U	Th	Pu
SRM 1566b			
Certified value/mg kg^{-1}	0.2550 ± (0.0014)	0.0367 ± (0.0043)	NC
Found: SN/mg kg^{-1}	0.2555 ± (0.0007)	0.0372 ± (0.0008)	$<12 \times 10^{-8}$
Found: LA/mg kg^{-1}	0.2532 ± (0.0009)	0.0348 ± (0.0013)	$<3 \times 10^{-8}$
Found: ETV/mg kg^{-1}	0.2545 ± (0.0020)	0.0363 ± (0.0023)	$<1.7 \times 10^{-8}$
SLRS-4			
Certified value/μg L^{-1}	0.050 ± (0.003)	0.018 ± (0.003)[b]	NC
Found: SN/μg L^{-1}	0.047± (0.002)	0.019 ± (0.002)	$<12 \times 10^{-5}$
Found: LA/μg L^{-1}	0.053 ± (0.005)	0.022 ± (0.007)	$<3 \times 10^{-5}$
Found: ETV/μg L^{-1}	0.049 ± (0.004)	0.020 ± (0.004)	$<1.7 \times 10^{-5}$
CASS-4			
Certified value/μg L^{-1}	3.05 ± (0.04)[a]	NC	NC
Found: SN/μg L^{-1}	3.03 ± (0.03)	0.0007 ± (0.0002)	$<12 \times 10^{-5}$
Found: LA/μg L^{-1}	3.02 ± (0.09)	0.0009 ± (0.0006)	$<3 \times 10^{-5}$
Found: ETV/μg L^{-1}	3.04 ± (0.07)	0.0004 ± (0.0002)	$<1.7 \times 10^{-5}$

[a] Information value only—isotope dilution results. [b] Information value only.[47] NC—not certified.

Table 5 Recovery studies for Pu ($n = 3$) (%)

Sample	Content	SN	LA	ETV
Standard solution	0.1 pg ml^{-1}	87 ± 13	97 ± 5	101 ± 3
	1 pg ml^{-1}	98 ± 3	100 ± 3	99 ± 2
Sea-water	0.1 pg ml^{-1}	88 ± 15	101 ± 4	98 ± 4
	1 pg ml^{-1}	101 ± 2	99 ± 3	99 ± 3
Oyster tissue	0.1 pg ml^{-1}	86 ± 16	98 ± 5	97 ± 4
	1 pg ml^{-1}	99 ± 3	100 ± 3	98 ± 3

Analytical results

The proposed methodology was validated by the analysis of several Certified Reference Materials for U and Th and by recovery of spikes of Pu added to these sample matrices. Results for the CRMs are summarized in Table 4 and are based on processing 3 replicate test samples. Good agreement between found and certified values is evident for all samples. Due to the high U and Th concentrations present in SRM 1566b, no $Ca_3(PO_4)_2$ co-precipitation was needed for the analysis of this sample.

The accuracy of the method for Pu was evaluated through spike recovery studies. Spikes of Pu added to DIW, sea-water and digested oyster tissue samples were subjected to the co-precipitation procedure. Two different final concentrations in the concentrates were studied: 0.1 and 1 pg ml^{-1}. Results are presented in Table 5 and are based on the analyses of 3 replicate samples subjected to preconcentration. Quantitative recoveries can be achieved using ETV and LA for the two different concentrations, independent of the sample. For SN, apparent recoveries were low when samples were spiked with 0.1 pg ml^{-1} due to measurement imprecision, as this concentration is close to the procedural LOD for this introduction system.

Conclusions

As amply supported by earlier publications addressing this topic, quantitation of low levels of radionuclides in environmental samples can be achieved using ICP-MS. The availability of several sample introduction methodologies provides the analyst with an enhanced measure of choice when considering such variables as total mass and/or volume of analyte available, concentration of dissolved solids present and relative concentrations of analyte to potential interferents (such as the problem presented by Pu and U, as UH).

Many laboratories are equipped with ETV units (used for graphite furnace atomic absorption) that can be adapted to use for sample introduction. Although this technique is very forgiving from the viewpoint of dissolved solids content and accommodates a large range of sample volume (up to 100 µl), incomplete vaporization and memory effects are not easily avoided when refractory actinides are the target analytes. Many popular variants of solution nebulization (with and without desolvation) are readily available but are limited in their ability to eliminate interferences arising from hydride formation and operate within narrow ranges of dissolved solids content, minimizing their ease of use with sample concentrates. LA of dried sample micro-droplets provides a relatively simple and reliable approach. Optimum performance, however, can only be elicited when dried droplet sizes are less than the focused beam diameter of the laser. As such, the expanded beam properties of the UP266 Macro system are well suited to this methodology. Use of electrospray[45] or microwave-assisted deposition/drying methods[46] may reduce sample residue size and improve performance when using systems having limited laser beam diameters. Reduced hydride formation (2 orders of magnitude) makes LA particularly attractive for the quantitation of these actinides.

Acknowledgements

This study was supported by the National Research Council Canada and the Chemical Radiological and Nuclear Research Technology Initiative (CRTI). The authors thank L. Neufeld of New Wave Research for the loan of the UP266MACRO laser ablation system used in this study and also J. Meija for the preparation of the illustrated contents list entry.

References

1 D. Desideri, M. A. Meli, C. Roselli, C. Testa, S. F. Boulyga and J. S. Becker, *Anal. Bioanal. Chem.*, 2002, **374**, 1091–1095.
2 E. Hrnecek, L. A. D. Heras and M. Betti, *Radiochim. Acta*, 2002, **90**, 721–725.
3 L. L. W. Kwong, J. Gastaud, J. La Rosa, S. H. Lee, P. P. Povinec and E. Wyse, *J. Radioanal. Nucl. Chem.*, 2004, **261**, 283–289.
4 S. Ohde, M. M. M. Hossain, H. Ozaki and T. Masuzawa, *J. Radioanal. Nucl. Chem.*, 2003, **258**, 275–280.
5 P. P. Povinec, J. J. La Rosa, S. H. Lee, S. Mulsow, I. Osvath and E. Wyse, *J. Radioanal. Nucl. Chem.*, 2001, **248**, 713–718.
6 S. H. Lee, J. Gastaud, J. J. La Rosa, L. L. W. Kwong, P. P. Povinec, E. Wyse, L. K. Fifield, P. A. Hausladen, L. M. Di Tada and G. M. Santos, *J. Radioanal. Nucl. Chem.*, 2001, **248**, 757–764.
7 J. S. Becker, *Spectrochim. Acta, Part B*, 2003, **58**, 1757–1784.
8 P. P. Povinec, *J. Radioanal. Nucl. Chem.*, 2005, **263**, 413–417.
9 M. V. Zoriy, L. Halicz, M. E. Ketterer, C. Pickhardt, P. Ostapczuk and J. S. Becker, *J. Anal. At. Spectrom.*, 2004, **19**, 362–367.
10 A. E. Eroglu, C. W. McLeod, K. S. Leonard and D. McCubbin, *Spectrochim. Acta, Part B*, 1998, **53**, 1221–1233.
11 R. S. Pappas, B. G. Ting and D. C. Paschal, *J. Anal. At. Spectrom.*, 2004, **19**, 762–766.
12 J. S. Becker, R. S. Soman, K. L. Sutton, J. A. Caruso and H. J. Dietze, *J. Anal. At. Spectrom.*, 1999, **14**, 933–937.
13 N. Berryman and T. Probst, *Radiochim. Acta*, 1997, **76**, 191–195.
14 M. Song and T. U. Probst, *Anal. Chim. Acta*, 2000, **413**, 207–215.
15 J. S. Alvarado and M. D. Erickson, *J. Anal. At. Spectrom.*, 1996, **11**, 923–928.
16 M. Song, T. U. Probst and N. G. Berryman, *Fresenius' J. Anal. Chem.*, 2001, **370**, 744–751.
17 P. Grinberg, S. N. Willie and R. E. Sturgeon, *J. Anal. At. Spectrom.*, 2005, **20**, 717–723.
18 J. S. Becker, C. Pickhardt and H. J. Dietze, *Int. J. Mass Spectrom.*, 2000, **202**, 283–297.
19 J. S. Becker and H. J. Dietze, *Fresenius' J. Anal. Chem.*, 1999, **365**, 429–434.
20 J. S. Becker, M. Zoriy, C. Pickhardt and M. Przybylski, *J. Anal. At. Spectrom.*, 2004, **19**, 149–152.
21 M. Legrand, R. Lam, M. Jensen Fontaine, E. D. Salin and H. M. Chan, *J. Anal. At. Spectrom.*, 2004, **19**, 1287–1288.
22 S. F. Boulyga, M. Tibi and K. G. Heumann, *Anal. Bioanal. Chem.*, 2004, **378**, 342–347.
23 Y. L. Lee, C. C. Chang and S. J. Jiang, *Spectrochim. Acta, Part B*, 2003, **58**, 523–530.
24 P. Goodall and S. G. Johnson, *J. Anal. At. Spectrom.*, 1996, **11**, 469–478.
25 J. S. Becker, C. Pickhardt and H. J. Dietze, *J. Anal. At. Spectrom.*, 2001, **16**, 603–606.
26 J. S. Becker, C. Pickhardt and W. Pompe, *Int. J. Mass Spectrom.*, 2004, **237**, 13–17.

27 M. Tibi and K. G. Heumann, *J. Anal. At. Spectrom.*, 2003, **18**, 1076–1081.
28 H. Falk, B. Hattendorf, K. Krengel-Rothensee, N. Wieberneit and S. L. Dannen, *Fresenius' J. Anal. Chem.*, 1998, **362**, 468–472.
29 E. F. Cromwell and P. Arrowsmith, *Anal. Chem.*, 1995, **67**, 131–138.
30 J. Stix, G. Gauthier and J. N. Ludden, *Can. Mineral.*, 1995, **33**, 435–444.
31 D. Gunther, I. Horn and B. Hattendorf, *Fresenius' J. Anal. Chem.*, 2000, **368**, 4–14.
32 J. Gonzalez, X. L. Mao, J. Roy, S. S. Mao and R. E. Russo, *J. Anal. At. Spectrom.*, 2002, **17**, 1108–1113.
33 L. Yang, R. E. Sturgeon and Z. Mester, *Anal. Chem.*, 2005, **77**, 2971–2977.
34 E. Denoyer, *At. Spectrosc.*, 1994, **15**, 7–16.
35 L. P. Colletti and G. J. Havrilla, *Adv. X-Ray Anal.*, 1997, **42**, 64–73.
36 D. B. Aeschliman, S. J. Bajic, D. P. Baldwin and R. S. Houk, *J. Anal. At. Spectrom.*, 2003, **18**, 872–877.
37 M. D. Seltzer and K. H. Berry, *Sci. Total Environ.*, 2005, **339**, 253–265.
38 G. Ertas and J. A. Holcombe, *J. Anal. At. Spectrom.*, 2005, **20**, 687–695.
39 M. Resano, M. Verstraete, F. Vanhaecke and L. Moens, *J. Anal. At. Spectrom.*, 2001, **16**, 1018–1027.
40 J. D. Venable, M. Detwiler and J. A. Holcombe, *Spectrochim. Acta, Part B*, 2001, **56**, 1697–1706.
41 M. J. Stump, R. C. Fleming, W.-H. Gong, A. J. Jaber, J. J. Jones, C. W. Surber and C. L. Wilkins, *Appl. Spectrosc. Rev.*, 2002, **37**, 275–303.
42 V. Vais, C. S. Li and J. Cornett, *J. Anal. At. Spectrom.*, 2004, **19**, 1281–1283.
43 B. G. Ting, R. S. Pappas and D. C. Paschal, *J. Anal. At. Spectrom.*, 2003, **18**, 795–797.
44 S. F. Boulyga, C. Testa, D. Desideri and J. S. Becker, *J. Anal. At. Spectrom.*, 2001, **16**, 1283–1289.
45 J. Axelsson, A.-M. Hoberg, C. Waterson, P. Myatt, G. L. Chield, J. Varney, D. M. Haddleton and J. Derrick, *Rapid Commun. Mass Spectrom.*, 1997, **11**, 209–213.
46 D. D. Link, H. M. Kingston, G. J. Havrilla and L. P. Colletti, *Anal. Chem.*, 2002, **74**, 1165–1170.
47 D. Yeghicheyan, J. Carignan, M. Valladon, M. B. Le Coz, F. Le Cornec, M. Castrec Rouelle, M. Robert, L. Aquilina, E. Aubry, C. Churlaud, A. Dia, S. Deberdt, B. Dupr, R. Freydier, G. Gruau, O. Henin, A. M. de Kersabiec, J. Mace, L. Marin, N. Morin, P. Petitjean and E. Serrat, *Geostand. Newsl.*, 2001, **25**, 465–474.

